Fabrication of elastic composite hydrogels using surface-modified cellulose nanofiber as a multifunctional crosslinker

Ryosuke Kobe,[1] Kouzou Yoshitani,[2] Yoshikuni Teramoto[2]

[1]Graduate School of Applied Biological Sciences, Gifu University, Gifu 5011193, Japan
[2]Faculty of Applied Biological Sciences, Gifu University, Gifu 5011193, Japan
Correspondence to: Y. Teramoto (E-mail: teramoto@gifu-u.ac.jp)

ABSTRACT: We fabricate composite hydrogels using surface-modified cellulose nanofiber (CNF) and *N*-isopropylacrylamide (NIPAm) as a multifunctional crosslinker and monomer, respectively. We expect to produce unique network structures that lead to elastomeric properties rarely reported for CNF-based materials. The modification of CNF is performed to introduce polymerizable vinyl groups onto the surface of CNF via condensation between the surface hydroxyl groups and 3-(trimethoxysilyl)propylmethacrylate. The modification and morphology of the surface-modified CNF (mCNF) are confirmed by FTIR, solid-state NMR, and FE-SEM, respectively. We conduct in situ radical polymerization under various conditions using mixtures of the mCNF aqueous suspension, NIPAm monomer, radical initiator, and catalyst. The mechanical properties of the obtained hydrogels (water content = 90 wt %) are evaluated. The gels can be elastically stretched to more than 700 times their original lengths and exhibit an apparent shape recovery with a small permanent deformation ($\sim$1/5 of the applied deformation under the gravity field). © 2015 Wiley Periodicals, Inc. J. Appl. Polym. Sci. **2016**, *133*, 42906.

INTRODUCTION

Cellulose nanofiber (CNF) or nanofibrillated cellulose attracts considerable attention in the broad field of material science and technology.[1] The bioderived nanofibers are favorable because of not only their abundance, biodegradability, and renewability but also their fine structure and excellent physical properties associated with the highly crystalline nature. For example, CNF is characterized by a large surface area ($\sim$800 m^2 g^{-1}),[2] high strength (2–3 GPa),[3] high elastic modulus ($\sim$140 GPa),[4–7] and low linear expansion coefficient (0.1 ppm K^{-1}).[8,9] Recently, several Japanese companies have industrialized CNF production, and developing uses for CNF has become a national project. One of the key approaches used to expand the application of CNF is material functionalization via diverse multicompositions.[9–13]

Considering the record of cellulosic composites, previous studies[14,15] demonstrated that highly compatible blends of some pairs of cellulose/synthetic polymers could be obtained using a suitable nonaqueous solvent, despite the generally believed intractability of natural fibrous polysaccharide, which shows poor solubility in most organic solvents. These previous studies indicated that strong intermolecular interactions that are superior or comparable with the self-associating nature of the respective components are indispensable for intimate mixing. As an alternative method to form unique microcomposites of cellulose, Nishio and Miyashita *et al.* developed the chemical blending technique of solution coagulation/bulk polymerization.[16–18] The in situ polymerization of a vinyl monomer as a coagulant and/or impregnant to form cellulose gel is an essential part of the reported method and enables us to obtain an interpenetrating network (IPN) of cellulose and synthetic polymer.

In recent years, several significant achievements have further progressed the IPN concept; these accomplishments include the creation of new classes of hydrogels (topological gel,[19] double-network gel,[20] tetra-PEG gel,[21] nanocomposite [NC] gel[22,23]) with good mechanical performance via ingenious combinations of polymeric matters. In particular, NC gel was synthesized by Haraguchi via the in situ polymerization of a vinyl monomer in the presence of clays as a multifunctional (an abundance of vinyl groups) polymer crosslinking agent; the obtained gel involved a polymer with homogeneously dispersed clay sheets.[22,23] Conventional organic crosslinked polymeric hydrogels exhibit mechanically weak and brittle natures because the inter-crosslinking molecular weight M_c (i.e., the chain length between crosslinking points) generally has a broad distribution.[22] Meanwhile, in the NC gel, the M_c is large, and its distribution is narrow. By extension, the flexible polymer chains between the clay sheets in the NC gels should have the ability to be extensively elongated and reversed without breaking the
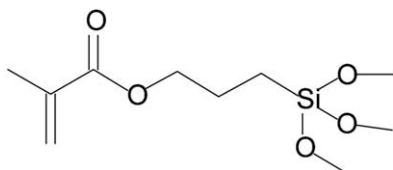
Scheme 1. Structural formula of MPS.

short polymer chains. As a result, the NC gels show extraordinary mechanical properties with high strength and elongations at break in excess of 1000%.

In this study, we investigated the fabrication of CNF-based stretchable composite hydrogels by combining surface-modified CNF (mCNF) and N-isopropylacrylamide (NIPAm) as a multifunctional crosslinking agent and monomer, respectively. Even though NC-type composite materials based on nanocelluloses have proposed by several groups,[24,25] we expect to achieve unique microstructures leading to high elasticity rarely reported for CNF-based materials. The mCNF crosslinker with vinyl groups was prepared via the condensation reaction between the surface hydroxyl groups of CNF and a silane coupling agent (3-(trimethoxysilyl)propylmethacrylate) (MPS). The incorporation of MPS and the surface morphology were confirmed by FTIR, solid-state NMR, and field-emission scanning electron microscopy (FE-SEM), respectively. The in situ radical polymerization was subsequently carried out by mixing the mCNF aqueous suspension, NIPAm monomer, potassium peroxodisulfate (KPS), and N,N,N',N'-tetramethylenediamine (TEMED) under various conditions. The hydrogels obtained in this manner contained approximately 90 wt % water and were evaluated for their mechanical and thermal transition properties. The hydrogels could be extended more than 700-fold without fracturing and displayed apparent restitution.

EXPERIMENTAL

Materials

CNF (BiNFi-s, WMa-100) was obtained as a 2-wt % water suspension from Sugino Machine. Characteristics of the CNF according to the brochure of the manufacturer are as follows: the average fiber diameter, 20–50 nm; degree of polymerization of cellulose, 200; viscosity, 3000 mPa s (25°C). NIPAm and N,N-dimethylacetoamide (DMAc) were purchased from Wako Pure Chemical Industries. NIPAm was purified by two recrystallizations from n-hexane and dried under vacuum at 30°C for 1 h. DMAc was dried by potassium hydroxide pellets before use. MPS (Scheme 1) was purchased from Sigma Aldrich. Other reagents were obtained from Wako Pure Chemical Industries and used without further purification.

Surface Modification of CNF

The as-provided CNF aqueous suspension was treated by a successive solvent exchange technique using acetone and DMAc at room temperature. The obtained suspension in DMAc (0.285 g in 100 mL) was introduced into a four-necked flask equipped with a mechanical stirrer under nitrogen flow (200 mL min^{-1}). The flask was then immersed in an oil bath thermoregulated at 100°C under stirring, and 3 mL of MPS was then added into the system. Continuous stirring was conducted for 18 h, which

is defined as the reaction time for silane coupling. The resulting suspension of fibrous product (mCNF) was subjected to successive solvent exchange using acetone and deionized water to give an actual mCNF concentration of 2 wt %.

Synthesis of Hydrogels

Hydrogels were prepared using initial suspension mixtures consisting of monomer (NIPAm), crosslinker (mCNF), diluent (deionized water), initiator (KPS), and catalyst (TEMED). Various concentrations of mCNF dispersion were prepared in a glass tube by adding deionized water and homogenized with a homogenizer (Physcotron NS-20G/20P, Microtec) at 3000 rpm for 30 min. The mCNF aqueous dispersion (26 g) was mixed with NIPAm (3 g) under vigorous stirring with a magnetic stirrer (40 rpm). Subsequently, both the initiator (0.03 g KPS in 1.5 mL H$_2$O) and catalyst (TEMED, 24 μL) were added into the mixture under stirring. The above procedures were all performed in an ice bath shielded from light. Free-radical polymerization was then allowed to proceed in an ethanol bath at 20°C for 20 h. To prepare specimens for tensile testing, the mixture containing all the ingredients was transferred into a polyethylene tube (5 mmφ) before polymerization. Oxygen was excluded from the system throughout the synthesis by a continuous flow of nitrogen (200 mL min^{-1}). Scheme 2 illustrates the preparation procedure of the mCNF and composite hydrogels.

Characterization

Surface Modification of CNF. *FTIR.* FTIR was carried out at the Division of Instrumental Analysis, Life Science Research Center, Gifu University. Spectra were recorded on a PerkinElmer Spectrum 100 FTIR apparatus over the wavenumber range of 400–4000 cm^{-1} at a resolution of 4 cm^{-1} via the accumulation of 32 scans. A standard KBr-pellet method was used for all the measurements and samples. To estimate the MPS content in mCNF, mixtures of CNF/MPS (MPS content: 5–30 wt %) were analyzed, and a calibration curve was constructed.

Solid-state ^{13}C CP/MAS NMR. Solid-state NMR experiments were carried out at 20°C with a JEOL ECA-500 equipped with a JEOL NM-93030 operated at a ^{13}C frequency 125 MHz, using the freeze-dried samples of CNF and mCNF. ^{13}C CP/MAS spectra were acquired with a spinning rate of 12 kHz, a contact time of 2 ms, a recycle delay time of 5 s, and 5000 FID signal accumulations. Assigned chemical shifts in ppm were 178 (CH*C*OO), 167 (CH$_2$=C*C*OO), 138 (*C*=CH$_2$), 126 (*C*H$_2$=C), 105 (pyranose C1), ~89 (pyranose C4), ~74 (pyranose C2/C3/C5), ~66 (O*C*H$_2$CH$_2$ and pyranose C6), 46 (SiO*C*H$_3$), 22 (OCH$_2$*C*H$_2$CH$_2$Si), 18 (*C*H$_3$C=C), and 9 (*C*H$_2$Si).

Field-emission scanning electron microscopy (FE-SEM). The morphologies of freeze-dried CNF and mCNF were observed by FE-SEM (S-4800, Hitachi High-Technologies) using an accelerating voltage of 1.5 kV at the Division of Instrumental Analysis, Life Science Research Center, Gifu University. The samples were coated with osmium for 20 s using a Neoc-Pro osmium coater (Meiwafosis) before observation.

Characterization of the CNF-Composite Hydrogel Samples. *Differential scanning calorimetry.* Differential scanning calorimetry (DSC) was carried out using a DSC7020 (Hitachi

a) Silane-CNF condensation

b) Hydrogel formation
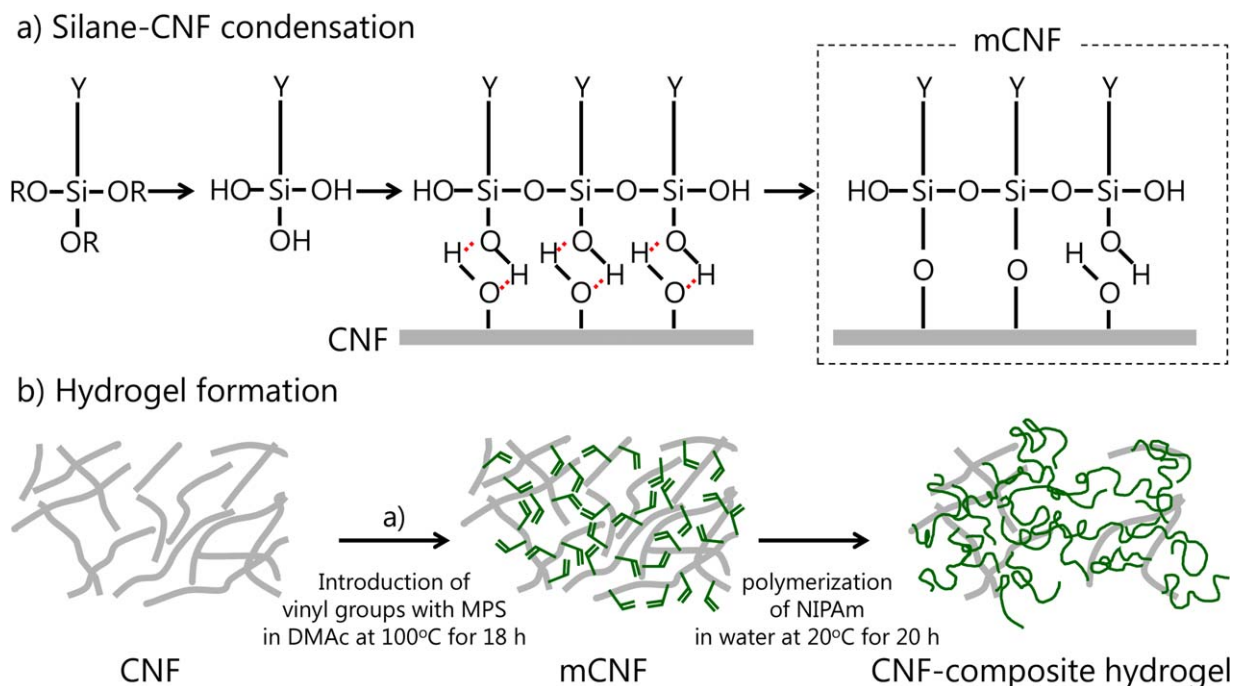
Scheme 2. Surface modification of CNF and hydrogel formation. [Color figure can be viewed in the online issue, which is available at wileyonlinelibrary.com.]

High-Technologies) with the following ordinary procedure. The samples (5 mg) were heated from 30°C to 200°C at a heating rate of 20°C min^{-1} and maintained at 200°C for 1 min. The samples were then rapidly cooled (at ~70°C min^{-1}) to 0°C. Subsequently, the samples were again heated to 200°C at a heating rate of 20°C min^{-1}.

Tensile testing. Tensile mechanical testing of hydrogel samples containing cylindrically shaped mCNF (5 mmφ × 21 mm length) was conducted using a compact table-top universal tester EZ-L (Shimadzu Corporation) under the following conditions: sample length between jaws, 1 mm; crosshead speed, 1000 mm min^{-1}; test temperature, 20°C. The initial cross-section (19.63 mm^2) was used to calculate the tensile strength and tensile moduli.

Elastomeric properties. Elastomeric properties were explored at 20°C using a hand-cranked drawing device (IMC-16AA, Imoto Machinery). Each of cylinder-shaped specimens (5 mmφ × 21 mm length) was fixed at the initial span length of 10 mm (L_0) onto the drawing device that was put vertically. The specimen was then uniaxially stretched to the desired length (L_1; L_1 = 30, 50, 100, and 200 mm) at 180 mm min^{-1}. The deformation state was maintained for 5 min. Subsequently, the bottom edges of the samples were cut and allowed to stand for 5 min. Finally, the lengths (L_2) of the specimens contracted. The applied and permanent distortions of the hydrogel specimens were calculated as D_{Appl} and D_{Perm}, respectively, from the following equations

$$D_{Appl} = \frac{L_1 - L_0}{L_0} \qquad (1)$$

$$D_{Perm} = \frac{L_2 - L_0}{L_0} \qquad (2)$$

RESULTS AND DISCUSSION

Surface Modification of CNF

The mCNF was obtained as a fibrous, opaque, white suspension in water, similar to the original CNF material provided as an aqueous fluid suspension. The structure of mCNF was characterized using FTIR, solid-state ^{13}C CP/MAS NMR, and FE-SEM.

The FTIR spectra for the original CNF, mCNF, and MPS are illustrated in Figure 1. For the original CNF and mCNF, two major adsorption bands were observed at 3100–3500 cm^{-1} and 2800–3000 cm^{-1}, which was ascribed to the O—H and —CH stretching vibration bands, respectively. On the other hand, for mCNF and MPS, a specific adsorption band at 1721 cm^{-1} was observed, which was assigned to the C═O stretching vibration of
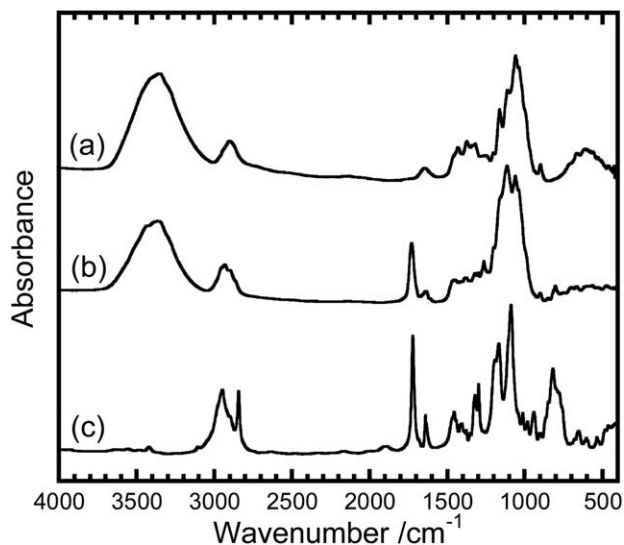
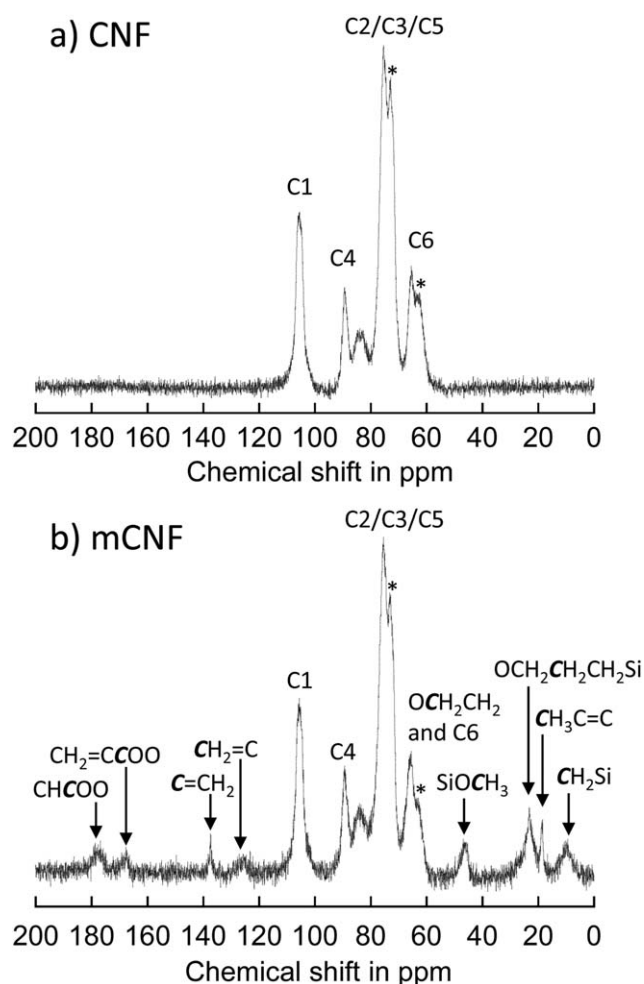**Figure 1.** FTIR spectra of (a) CNF, (b) mCNF, and (c) MPS.

Figure 2. Solid-state ^{13}C CP/MAS spectra for (a) CNF and (b) mCNF.

other hand, by mutual comparison of the spectra of the CNF and mCNF, there is a possibility that the modification of the hydroxyl groups of the CNF by MPS is related to the different intensity ratios for the split signals (marked with asterisk in Figure 2) of the pyranose carbons [$\sim$74 (C2/C3/C5) and $\sim$66 (C6) ppm].

FTIR is useful in the analysis of polysaccharide nanofibers due to its limited solubility in solvents. Nevertheless, FTIR requires calibration unlike the absolute techniques such as NMR, which permits the direct determination of the chemical compositions of soluble cellulosics. We thus determined the degree of modification of the synthesized mCNF by constructing a calibration curve using mixtures of CNF and MPS. Figure 3 shows an example FTIR spectrum of a mixture of CNF/MPS; the baselines for the probe (C=O of MPS) and internal reference (CNF) absorptions range from 1800 to 1600 cm^{-1} and 1320 to 860 cm^{-1}, respectively. The internal reference absorption centered at 1038 cm^{-1} corresponds to the C—O stretching in cellulose. Therefore, the absorption ratio A_{MPS}/A_{CNF} can be taken as a measure of the change in chemical composition of the mCNF. Figure 4 displays the results of monitoring the absorption ratio for the mixtures of CNF and MPS. A calibration curve ($y = 0.0111x + 0.0851$, $R^2 = 0.935$) was constructed via linear regression. Consequently, the degree of modification of the mCNF was calculated with the following equation in terms of the commonly used molar substitution (MS), which is defined as the average number of introduced polymerized MPS (PMPS) units per anhydroglucose residue of CNF

$$MS = \frac{162 \times \left(\frac{A_{MPS}/A_{CNF} - 0.0851}{0.111}\right)}{248 \times 100 \times \left(1 - \frac{A_{MPS}/A_{CNF} - 0.0851}{0.111}\right)} \qquad (3)$$

the carbonyl group of the MPS moiety. The adsorption bands of the Si—O—Si bonds of the siloxane compounds in the range of 1000–1130 cm^{-1} appeared to be overlapped by the cellulosic bands due to C—O bending modes. Even though no affirmative evidence of covalent bonding (Si—O—C) between CNF and MPS was obtained from Figure 1, the mCNF apparently contained the MPS moiety, as demonstrated by the existence of the C=O stretching vibration even after the mCNF was subjected to an intensive purification process.

Solid-state NMR spectroscopy gave some additional information. Figure 2 shows the solid-state ^{13}C CP/MAS spectra of the original CNF and mCNF. In the spectrum of the mCNF, we can see the signals assigned to the vinyl units 138 ppm (*C*=CH$_2$) and 126 ppm (*C*H$_2$=C) of the MPS moiety, which indicates that the mCNF can act as the macromonomer for vinyl polymerization. The occurrence of polycondensation of MPS monomers and/or condensation of MPS with the surface hydroxyl groups of CNF can be confirmed by the relatively small signal of SiO*C*H$_3$ (46 ppm), which should be originally come down to the three carbons of the methoxy groups of the MPS monomer, even though the spectra are not adequate for the quantitative characterization. In addition, because there was a signal assigned to CH*C*OO at 178 ppm, part of the MPS units in the mCNF was the form vinyl-polymerized. On the
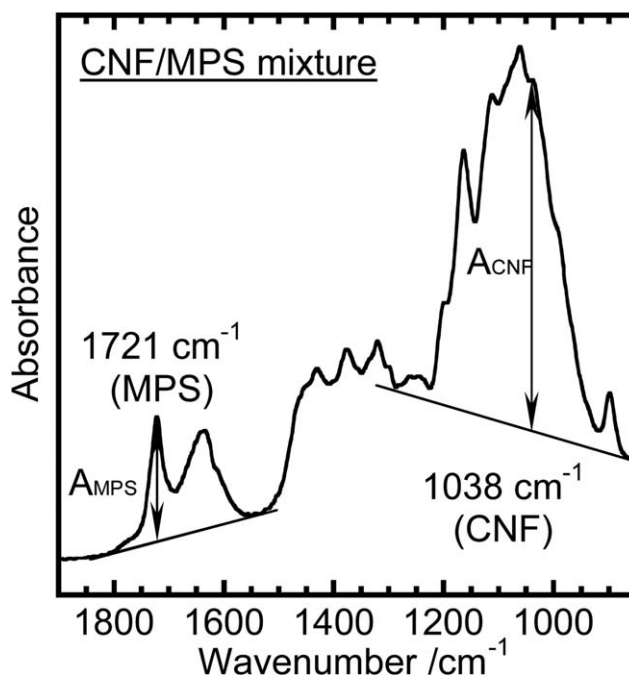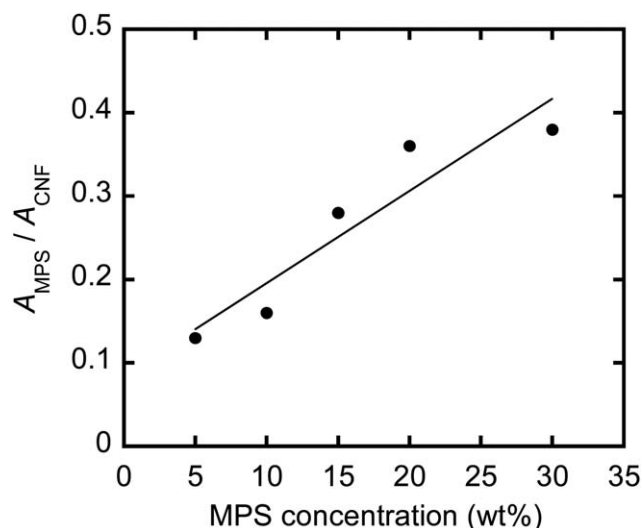

Figure 3. An example FTIR spectrum of the mixture of CNF/MPS (85/15 in weight).

Figure 4. The FTIR absorption ratios, A_{MPS}/A_{CNF}, for mixtures of CNF and MPS with different MPS concentrations.

where the numbers 162 and 248 denote the molecular weights of the repeating unit of cellulose and PMPS, respectively, and 0.0851 and 0.111 are the intercept and slope of the linear fitting in Figure 4, respectively. By applying eq. (3), MS was determined to be 0.30. The parameter MS was adopted because this structural parameter is a convenient index to identify the modification degree, even though only the surface hydroxyl groups of CNF were supposed to participate in the present silane coupling reaction. We estimated that the MS value of 0.30 indicated the incorporation of appreciable amounts of MPS units into the mCNF surface.

Figure 5 shows typical FE-SEM micrographs of the original CNF and mCNF. The mean diameter of the original CNF [Figure 5(a)] was calculated to be 30 nm by averaging the dimensions of 50 fibers. On the other hand, the micrograph of mCNF is shown in Figure 5(b); we can see numerous nanostructures apparently attached to the surface of CNF. The nanostructures can be ascribed to the polymerized product of MPS, namely, PMPS. The polymerization of MPS was confirmed by solid-state ^{13}C CP/MAS spectrum of the mCNF. Because no aggregates of nanostructures without nanofibrous skeletons derived from
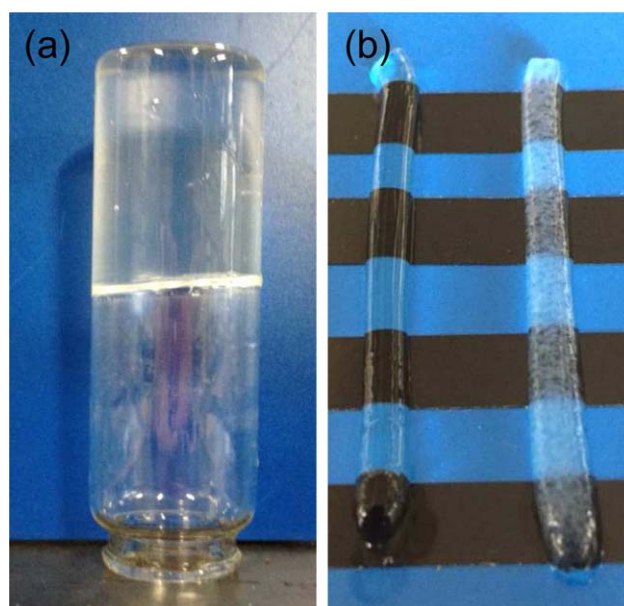

Figure 6. Visual appearances of the CNF composite hydrogels containing various contents of mCNF: (a) 0.05 wt % and (b) 0.01 wt % (left) and 0.1 wt % (right). [Color figure can be viewed in the online issue, which is available at wileyonlinelibrary.com.]

CNF were observed in this study, it is highly probable that the PMPS was chemically adhered to the CNF surface.

Characterization of the CNF–Composite Hydrogels
Visual Appearance and Temperature Response. Figure 6 illustrates the visual appearances of the CNF–composite hydrogels prepared by the polymerization of NIPAm monomer in the presence of mCNF suspended in water. As shown in Figure 6(a), the obtained hydrogels lost fluidity and appeared transparent when low concentrations (<0.1 wt %) of mCNF were incorporated. In comparison with this, if the polymerization of NIPAm was conducted in the presence of the original unmodified CNF, the product was a high-viscosity aqueous liquid (PNIPAm solution) with suspending CNF. Since the mCNF precursor did not finely disperse in water, the hydrogels containing ≥ 0.1 wt % mCNF appeared opaque [Figure 6(b)]. On the other hand, the products obtained via NIPAm
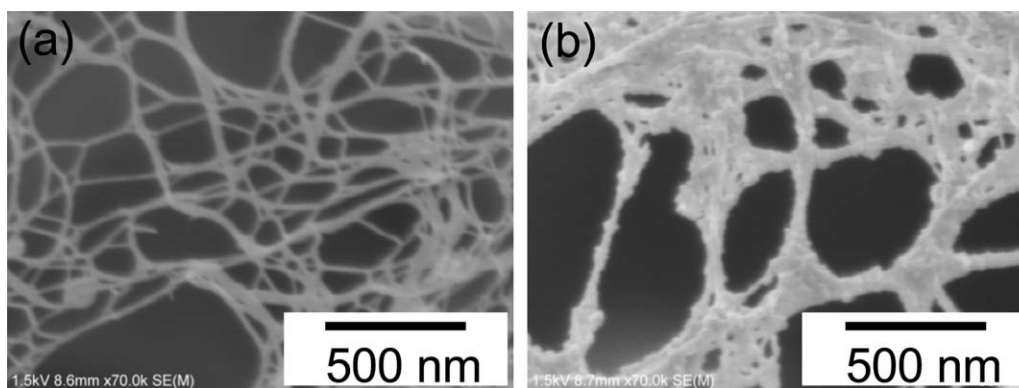
**Figure 5.** FE-SEM images of (a) CNF and (b) mCNF.

polymerization in the presence of unmodified CNF exhibited a fluidic nature, indicating that no gelation state based on cross-linking formation existed; instead, the product was simply a mixture of the original CNF and an aqueous solution of free PNIPAm chains. When the CNF–composite hydrogels were subjected to hot air from a hair dryer, the originally transparent hydrogels quickly became cloudy. This effect is attributed to the coil–globule transition of the PNIPAm component; thus, we qualitatively confirmed the temperature-responsive property of the CNF–composite hydrogels.

Estimation of Crosslinking State. To estimate the degree of crosslinking, we defined a quantitative relationship between the functional groups and reagents used to synthesize the CNF–composite hydrogels (mentioned in the Experimental section). The MS of the mCNF was determined to be 0.30 by FTIR. The content of MPS units introduced into the mCNF (w_{MPS} in wt %) can thus be calculated as

$$w_{MPS} = \frac{248 \times MS}{162 + 248 \times MS} \times 100 \qquad (4)$$

where the numbers 162 and 248 denote the molecular weights of the repeating units of cellulose and PMPS, respectively. The w_{MPS} for the mCNF used as the starting material in this study was determined to be 31.5 wt %. In the final hydrogel products (30.5 g) containing 0.005, 0.01, 0.05, and 0.1 wt % mCNF, the amounts of MPS included were 1.9, 3.9, 19, and 39 μmol, respectively, which were equal the amounts of vinyl groups (C=C). The molar ratios (NIPAm/C=C) of the in-feed NIPAm (3 g, 26.5 mmol) to C=C of MPS were thus determined to be 1.3×10^4, 6.8×10^3, 1.4×10^3, and 6.8×10^2 for the hydrogels incorporating 0.005, 0.01, 0.05, and 0.1 wt % of mCNF, respectively. To calculate actual values of the inter-crosslinking molecular weight M_c (i.e., the chain length between crosslinking points) of the PNIPAm chains, we need more structural information such as the fractions of the PNIPAm chains included in the crosslinking structure, grown as the grafting ones, and homopolymerized ones. However, it is safe to conclude that the NIPAm/C=C molar ratios ($6.8 \times 10^2 - 1.3 \times 10^4$) were sufficiently large to achieve the incorporation of flexible PNIPAm chains in the CNF–composite hydrogels.

To obtain further insights into the degree of crosslinking, we characterized the thermal transition behaviors of the freeze-dried gel samples using DSC. According to the literature,[23] linear PNIPAm synthesized by ordinary radical homopolymerization exhibits a glass transition temperature (T_g) of 142°C. On the other hand, it is well known that crosslinking increases T_g by introducing restrictions on the molecular motions of chains.[26] For example, the T_g values for conventional chemically crosslinked PNIPAm samples randomly copolymerized with a divinyl monomer such as N,N'-methylenebis(acrylamide) were reported to gradually increase with increasing crosslinker concentration.[23] The T_g values of the dried samples of the present CNF composite hydrogels were determined to be 138–141°C, which are comparable to or lower than that of linear PNIPAm. We can thus assume that the M_c was sufficiently high in the CNF composite hydrogel samples formed by the present syn-
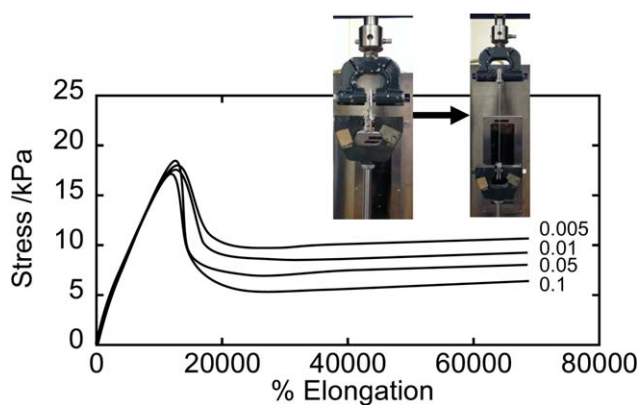
Figure 7. Stress–strain curves for cylinder-shaped (5 mmφ) hydrogel specimens containing different amounts of mCNF. The numbers in the figure represent the mCNF concentrations (wt %). The inset photos show the appearances of the samples in a tensile machine. [Color figure can be viewed in the online issue, which is available at wileyonlinelibrary.com.]

thetic procedure, indicating that there were small numbers of crosslinking points in the hydrogels.

Mechanical Properties

Stress–Strain Curves from the Tensile Tests of the Hydrogel Specimens. Figure 7 shows the stress–strain curves obtained at 23°C for the cylinder-shaped (5 mmφ) hydrogel specimens containing different amounts of mCNF. It should be noted that all the hydrogel specimens were highly extendable and could be elongated to more than 70,000% of elongation, irrespective of the mCNF content. In fact, we could only obtain elongation data for % elongation $\leq \sim 70,000\%$ due to instrumental constraints (the limiting displacement was 700 mm for the initial span length of 1 mm); thus, the hydrogel specimens may be able to be stretched more. Considering such a large elongation, we must consider the possibility of partial specimen rupture during tensile testing. However, no apparent fracturing was observed, and the cylindrical specimens were uniformly deformed. We can therefore conclude that the present hydrogel samples are highly stretchable materials from a practical point of view, which is attributed mainly to the high M_c, the chain length between crosslinking points, as was suggested above. In addition, there is a possibility for the large elongation given rise to by secondary forces such as hydrogen bondings and entanglements between PNIPAm chains and between mCNFs, where these forces might act as the physical crosslinking points. The possible increase in the degree of intermolecular interactions can be ascribed to the high molecular weight of PNIPAm.

The maximum tensile strength and Young's modulus were estimated to be about 18 kPa and 35 Pa, respectively, for all hydrogel samples. Haraguchi et al.[23] reported that the clay-based NC gel containing 1-wt % clay exhibited 27 kPa, 840 Pa, and 1308% of tensile strength, Young's modulus, and elongation, respectively; we interpret that the more ductile nature of the present CNF-based composite gel samples is mainly due to the lower contents of the multifunctional crosslinker (≤ 0.1 wt %). On the other hand, the applied stress of the specimens in the highly stretched state (% elongation $\geq \sim 20,000\%$) decreased with increasing mCNF content. This may be because of the
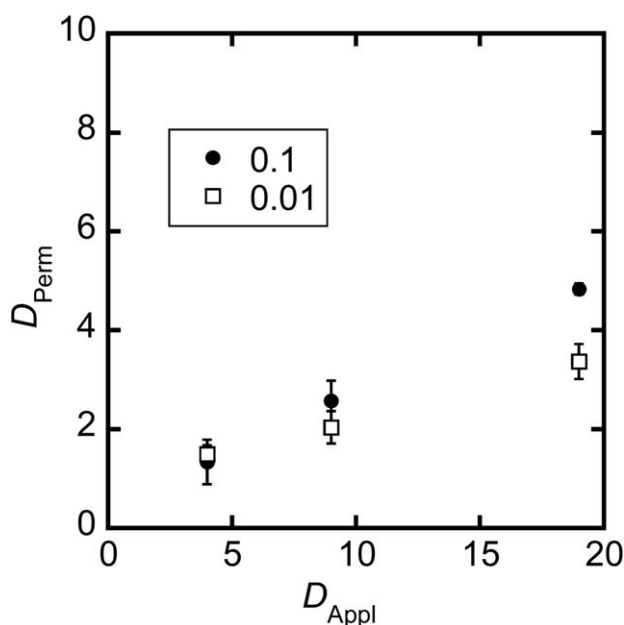
Figure 8. Extension–contraction behaviors of the cylinder-shaped (5 mmφ) CNF-composite hydrogel specimens containing different amounts of mCNF. The applied and permanent distortions (D_{Appl} and D_{Perm}) are plotted. The legend shows the mCNF concentrations (wt %).

high frequency of occurrence of partial rupture due to the low dispersibility of mCNF in the hydrogel samples (originally in water), which is a possible cause of mechanical defects.

Elastomeric Behavior. The elastomeric properties of the cylinder-shaped hydrogel samples (mCNF concentration = 0.1 and 0.01 wt %) were investigated at 20°C using a vertically placed hand-cranked drawing device. The initial span length (L_0) was 10 mm. A hydrogel sample was loaded up to a certain stretch (L_1 = 30, 50, 100, and 200 mm), kept at that loading for 5 min, unloaded to zero force by cutting the lower end of the extended gel sample, and then left the specimen for 5 min under the gravitational force field. Subsequently, we measured the contracted length (L_2). Figure 8 displays the applied and permanent distortions (D_{Appl} and D_{Perm}) calculated from eqs. (1) and (2) (see Experimental section), respectively. As shown in Figure 8, the shapes of both hydrogel samples were restored to an appreciable extent after unloading. The retained permanent deformation after unloading was determined to be ~1/5 of the D_{Appl} under the gravity field. Such a permanent deformation can be attributed to internal damage, as was pointed in the interpretation of the stress–strain curves. It might be reasonable that the larger D_{Perm} values along with large displacements were observed for the hydrogel samples with higher mCNF content. This is because the high frequency of occurrence of partial rupture due to the low dispersibility of mCNF in the hydrogel samples as has been mentioned above. Nonetheless, the specimens showed clear contractional shape recovery behavior, which is ascribable to the elastomeric behavior of the crosslinked PNIPAm chains with large M_c. The above-mentioned secondary interactions such as hydrogen bondings and entanglements between PNIPAm chains and between mCNFs are also the possible driving force for the attainment of the ability of shape recovery.

CONCLUSIONS

In this study, we successfully fabricated elastomeric hydrogels (water content = ~90 wt %) comprising PNIPAm and mCNF, which was surface modified by silane coupling to introduce polymerizable vinyl groups. The maximum strain of the CNF–composite hydrogel products reached 700-fold at least. The specimens exhibited apparent retraction behavior. Such a high stretchability can be mainly attributed to the large inter-crosslinking molecular weight M_c of PNIPAm. The mCNF acted as an effective multifunctional crosslinking agent. Even though the orientation of rigid CNF should be sensitive to applied strain, we could not detect any evidence such as birefringence for the preferential orientation as highly stretching of flexible gel samples,[27–29] which was probably because of the low CNF contents in the composite gel samples. A more elaborate surface modification of CNF combining both the initiation ability of vinyl polymerization and dispersibility in the polymerization system would allow the more wide-ranging control of the mechanical performance and nanofiber orientation of the CNF–composite hydrogels, which is a subject of future investigation.

ACKNOWLEDGMENTS

REFERENCES

1. Klemm, D.; Kramer, F.; Moritz, S.; Lindstrom, T.; Ankerfors, M.; Gray, D. G.; Dorris, A. *Angew. Chem. Int. Ed.* **2011**, *50*, 5438.

2. Kobayashi, Y.; Saito, T.; Isogai, A. *Angew. Chem. Int. Ed.* **2014**, *53*, 10394.

3. Page, D. H.; El-Hosseiny, F. *J. Pulp Pap. Sci.* **1983**, *9*, 99.

4. Sakurada, I.; Nukushima, Y.; Ito, I. *J. Polym. Sci.* **1962**, *57*, 651.

5. Nishino, T.; Takano, K.; Nakamae, K. *J. Polym. Sci. Part B: Polym. Phys.* **1995**, *33*, 1647.

6. Matsuo, M.; Sawatari, C.; Iwai, Y.; Ozaki, F. *Macromolecules* **1990**, *23*, 3266.

7. Iwamoto, S.; Kai, W.; Isogai, A.; Iwata, T. *Biomacromolecules* **2009**, *10*, 2571.

8. Nishino, T.; Matsuda, I.; Hirao, K. *Macromolecules* **2004**, *37*, 7683.

9. Nogi, M.; Iwamoto, S.; Nakagaito, A. N.; Yano, H. *Adv. Mater.* **2009**, *2121*, 1595.

10. Yano, H.; Sugiyama, J.; Nakagaito, A. N.; Nogi, M.; Matsuura, T.; Hikita, M.; Handa, K. *Adv. Mater.* **2005**, *17*, 153.

11. Berglund, L. A.; Peijs, T. *MRS Bull.* **2010**, *35*, 201.

12. Qua, E. H.; Hornsby, P. R.; Sharma, H. S. S.; Lyons, G.; McCall, R. D. *J. Appl. Polym. Sci.* **2009**, *113*, 2238.

13. Fahma, F.; Hori, N.; Iwata, T.; Takemura, A. *J. Appl. Polym. Sci.* **2013**, *128*, 1563.

14. Nishio, Y. In Cellulose Polymers, Blends, and Composites; Gilbert, R. D., Ed.; Hanser: Munich, New York, **1994**, p 95.

15. Nishio, Y.; Haratani, T.; Takahashi, T.; Manley, R. S. *Macromolecules* **1989**, *22*, 2547.

16. Nishio, Y. *Adv. Polym. Sci.* **2006**, *205*, 97.

17. Miyashita, Y.; Nishio, Y.; Kimura, N.; Suzuki, H.; Iwata, M. *Polymer* **1996**, *37*, 1949.

18. Miyashita, Y.; Kobayashi, R.; Kimura, N.; Suzuki, H.; Nishio, Y. *Carbohydr. Polym.* **1997**, *34*, 221.

19. Okumura, Y.; Ito, K. *Adv. Mater.* **2001**, *13*, 485.

20. Gong, J. P.; Katsuyama, Y.; Kurokawa, T.; Osada, Y. *Adv. Mater.* **2003**, *15*, 1155.

21. Sakai, T.; Matsunaga, T.; Yamamoto, Y.; Ito, C.; Yoshida, R.; Suzuki, S.; Sasaki, N.; Shibayama, M.; Chung, U. I. *Macromolecules* **2008**, *41*, 5379.

22. Haraguchi, K.; Takehisa, T. *Adv. Mater.* **2002**, *14*, 1120.

23. Haraguchi, K.; Takehisa, T.; Fan, S. *Macromolecules* **2002**, *35*, 10162.

24. Aouada, F. A.; de Moura, M. R.; Orts, W. J.; Mattoso, L. H. *J. Agric. Food Chem.* **2011**, *59*, 9433.

25. Yang, J.; Han, C. R.; Duan, J. F.; Ma, M. G.; Zhang, X. M.; Xu, F.; Sun, R. S.; Xie, X. M. *J. Mater. Chem.* **2012**, *22*, 22467.

26. Nielsen, L. E. Mechanical Properties of Polymers and Composites; Marcel Dekker: New York, **1974**.

27. Murata, K.; Haraguchi, K. *J. Mater. Chem.* **2007**, *17*, 3385.

28. Wu, Z. L.; Sawada, D.; Kurokawa, T.; Kakugo, A.; Yang, W.; Furukawa, H.; Gong, J. P. *Macromolecules* **2011**, *44*, 3542.

29. Shikinaka, K.; Koizumi, Y.; Kaneda, K.; Osada, Y.; Masunaga, H.; Shigehara, K. *Polymer* **2013**, *54*, 2489.